



HAL
open science

A Matlab/Simulink model of the inner ear angular accelerometers sensors

Pierre Selva, Yves Gourinat, Joseph Morlier

► **To cite this version:**

Pierre Selva, Yves Gourinat, Joseph Morlier. A Matlab/Simulink model of the inner ear angular accelerometers sensors. ASME 2009 International Design Engineering Technical Conferences & Computers and Information in Engineering Conference, Aug 2009, San Diego, United States. pp.0. hal-01853232

HAL Id: hal-01853232

<https://hal.science/hal-01853232>

Submitted on 2 Aug 2018

HAL is a multi-disciplinary open access archive for the deposit and dissemination of scientific research documents, whether they are published or not. The documents may come from teaching and research institutions in France or abroad, or from public or private research centers.

L'archive ouverte pluridisciplinaire **HAL**, est destinée au dépôt et à la diffusion de documents scientifiques de niveau recherche, publiés ou non, émanant des établissements d'enseignement et de recherche français ou étrangers, des laboratoires publics ou privés.



This is a publisher-deposited version published in: <http://oatao.univ-toulouse.fr/>
Eprints ID: 3072

To cite this document: SELVA, Pierre. MORLIER, Joseph. GOURINAT, Yves. A Matlab/Simulink model of the inner ear angular accelerometers sensors. In: *ASME 2009 International Design Engineering Technical Conferences & Computers and Information in Engineering Conference*, 30 August - 02 Sept 2009, San Diego, USA.

Any correspondence concerning this service should be sent to the repository administrator: staff-oatao@inp-toulouse.fr

DETC2009-87166

A Matlab/Simulink model of the inner ear angular accelerometers sensors

Pierre Selva

Département Mécanique des Structures et Matériaux

Yves Gourinat

Département Mécanique des Structures et Matériaux

Joseph Morlier

Département Mécanique des Structures et Matériaux

Université de Toulouse, ISAE/DMSM

10 av. Edouard Belin BP54032, 31055 Toulouse, France

ABSTRACT

In order to keep tabs on the position and motion of our body in space, nature has given us a fascinating and very ingenious organ, the inner ear. Each inner ear includes five biological sensors - three angular and two linear accelerometers - which provide the body with the ability to sense angular and linear motion of the head with respect to inertial space. The aim of this paper is to present a mechanical model of the semicircular canals - which behave as angular accelerometers - in a specific kinematic environment. This model, implemented in Matlab/Simulink, simulates the rotary chair testing, which is one of the usual tests carried out during a diagnosis of the vestibular system. This model also allows to simulate several head rotations, and at the same time to show the state - excited or inhibited - of each angular sensors. Therefore, the developed model can be used as a learning and demonstrating tool either in the medicine field to understand the behavior of the sensors during any kind of motion or in the aeronautical field to relate the inner ear functioning to some sensory illusions. In addition, the first results also show the influence of the non-orthogonality of the canals on the sensors stimulation.

1. INTRODUCTION

The vestibular apparatus is located in the inner ear and is vital for our dynamic equilibrium. It constitutes a three dimensional inertial-guidance system. Since the 1950s, the advent of aerospace flight with its new demands has accelerated the pace of vestibular research. Furthermore, a full understanding of the mechanics of a healthy inner ear may contribute to the diagnosis and treatment of the vestibular part in a diseased state. This is the reason

several authors have studied the mechanics of the semicircular canals (SCC), which detect changes in angular acceleration. The first model regarding the canals was proposed by W. Steinhausen [1], and is known as the classical torsion pendulum system, which has been the benchmark for subsequent works (Groen [2], Van Egmond [3], Njeugna [4], Fernandez [5]). Since Steinhausen, several models based on the resolution of the fluid flow within the canals have been established (Oman [6], Rabbitt [7], Steer [8], Van Buskirk [9]). All these models lead to a transfer function between the output of each canal, i.e. the discharge of the afferent nerve fibers innervating the canals, and the angular acceleration of the head with respect to an inertial space.

The scope of this paper is to present a numerical model of the SCC in a kinematic environment. This model simulates the rotary chair testing, one of the procedures usually performed by specialists during a diagnosis of the vestibular system, which will be explained in-depth later in this paper. In order to achieve this goal, the model follows different steps. First, it solves the equations of motion in each coordinate system. Second, it computes the angular velocity vectors, which are then projected on the perpendicular of each canal plane. Third, the state of each sensor is derived according to their transfer function. A three-dimensional animation is also developed to visualize the state of each sensor in real time. After the introduction of the anatomy and

physiology of the sensory system, the modeling of a single-canal is presented. The kinematics problem is then formulated in the coordinate system attached to the canals. Finally, some numerical tests are performed.

2. ANATOMY AND PHYSIOLOGY OF THE SEMICIRCULAR CANALS

The vestibular system, which is also known as the organ of equilibrium, is located within the temporal region of the skull (in the inner ear), and consists of two specialized types of sensory systems: the semicircular canals - which respond to angular acceleration, and two otolith organs - which primarily detect changes in linear acceleration and gravity (Roman [10], Sauvage [11]).

These sensory systems consist of fluid-coupled structures that induce a motion-sensitive signal on the vestibular nerve. This signal is then transmitted to the nervous central system where other afferent systems such as vision and proprioception also converge for spatial orientation, postural stability and gaze stabilization. Anatomically, the semicircular canals consist bilaterally of three sets of membranous ducts suspended in a fluid called perilymph, and are oriented in almost mutually orthogonal planes (Figure 1).

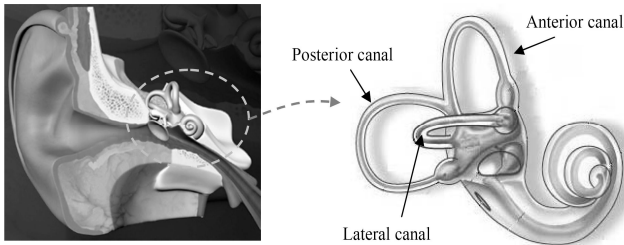


Figure 1: Global visualization of the inner ear and zoom on the 3 canals (angular sensors).

The membranous structure is filled with another Newtonian incompressible fluid called endolymph (Steer [8]). Each canal contains a gelatinous membrane known as the cupula that completely seals the semicircular canals (Hillman [12]). Angular motion sensation relies on inertial forces, caused by head accelerations, to generate endolymph fluid flow within the toroidal semicircular canals. More precisely, when the head rotates, the endolymph in the canals lags behind due to its inertia and produces a force across the cupula, deflecting it in the opposite direction of head movement. This deflection causes a sensation of motion. At a constant rotation rate,

the endolymph in the canals tends to catch up with the rotation of the head due to the viscosity, eliminating the relative movement. Eventually, as long as the rotation rate remains constant, the cupula returns to a vertical position due to its elastic properties, and the sensation of motion eventually ceases.

Because of the imperfect orthogonality of the canals, they all can be stimulated by any rotation. However, it has been shown that each canal admits a specific direction of stimulation, which maximizes the excitation (Rabbitt [13]).

3. MODELING

3.1 Single-canal macromechanics

Angular motion sensation relies on inertial forces, caused by head accelerations, to generate endolymph fluid flow within the toroidal semicircular canals. This fluid flow is described by the torsion pendulum model, which arises from the works of Steinhausen [1], Groen [2], and refined by Rabbitt [7]. It describes the semicircular canals as a second-order overdamped system governed by:

$$m \frac{d^2 Q}{dt^2} + c \frac{dQ}{dt} + kQ = f \quad (1)$$

where Q is the endolymph volume displacement. The term m represents the mass of the fluid contained in the canal, c describes the viscous damping appearing in the duct, and k defines the stiffness of the cupula, which behaves as a restoring spring against the direction of fluid displacement. f is an inertial forcing term defined by:

$$f = \oint \rho (\ddot{\Omega} \times R(s)) ds \quad (2)$$

where $\ddot{\Omega}$ is the angular acceleration of the head, and $R(s)$ is the local position vector of a point located on the streamline of the canal. In this model, the membranous semicircular canal is considered as a rigid-walled structure as its stiffness is largely higher than the stiffness of the cupula. A Poisson ratio of 0.48, close to usual considered value for incompressible material, is widely accepted for the cupula. Therefore, the cupula volume displacement can be approximated by the endolymph volume displacement.

Equation (1) is transformed to Laplace domain to obtain the transfer function $F_{scc}(s)$ between the cupula volume displacement Q_c and the angular head velocity $\dot{\Omega}$, so that:

$$F_{scc}(s) = \frac{Q_c}{\dot{\Omega}} = \frac{(d/m)s}{(s+1/\tau_1)(s+1/\tau_2)} \quad (3)$$

As the system is highly overdamped, the two time constants are approximated by $\frac{1}{\tau_1} \approx \frac{k}{c}$ and $\frac{1}{\tau_2} \approx \frac{c}{m}$. The

values that we use in the present model directly depend on the morphology of the canal and the physical properties of both the fluid and the cupula. For humans, these values are: $m=1070\text{g.cm}^{-4}$, $c=179 \text{ kg.s}^{-1}.\text{cm}^{-4}$, $k=13.3 \text{ kg.s}^2.\text{cm}^{-4}$, $d=0.76 \text{ g.cm}^{-1}$ (Rabbitt [7]).

3.2 Enhanced formulation of the kinematics problem

This work is based on the research of Adenot [14] who developed a model devoted to the analysis of the Coriolis Cross-Coupling Stimulus that was restricted to head coordinate frame. The objective of the present model is to simulate a real case of vestibular diagnosis carried out by a specialist, which takes into account the non-orthogonal coordinate system attached to the SCC. Figure 2 illustrates the usual procedure. The patient is strapped into a rotating chair, and experiences a rotational motion around an Earth vertical axis. Due to the inertia of the endolymph, the cupula inside the canal perpendicular to the axis of rotation is deflected. A perception of rotation results. The patient can also be made to undergo several head rotations in order to stimulate others canals.

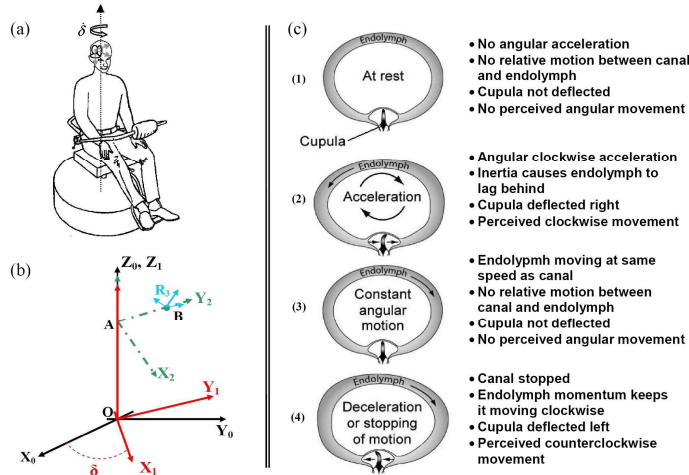


Figure 2: (a) Visualization of the diagnosis procedure, (b) Different coordinate systems : R_0 : $(O, \vec{X}_0, \vec{Y}_0, \vec{Z}_0)$ fixed orthogonal coordinate system, R_1 : $(O, \vec{X}_1, \vec{Y}_1, \vec{Z}_1)$ orthogonal coordinate system attached to the rotating chair, R_2 : $(A, \vec{X}_2, \vec{Y}_2, \vec{Z}_2)$ orthogonal coordinate system attached to the head, R_3 : $(B, \vec{X}_3, \vec{Y}_3, \vec{Z}_3)$ non-orthogonal coordinate system defined by the 3 perpendiculars of the semicircular canals, (c) effect of head rotation on the semicircular canals, the displacement of the cupula is plotted on figure 6 (a) or (b).

In the present model, the canals are assumed totally uncoupled, i.e. no fluid flow interactions between them are considered. Hence, a canal is stimulated if the component of the rotation vector along the perpendicular of this canal is non null.

The different coordinate frames are defined in Figure 2b. The movement of the coordinate frame R_1 relatively to R_0 is merely a rotation around a vertical axis, so that the angular velocity is given by $\vec{\omega}_{1/0} = \dot{\delta}\vec{z}_0 = \dot{\delta}\vec{z}_1$. The head angular velocity with respect to R_1 is given by $\vec{\omega}_{2/1} = \alpha\vec{X}_2 + \beta\vec{Y}_2 + \gamma\vec{Z}_2$, where α, β, γ are respectively the rotation angles around the axis \vec{X}_2, \vec{Y}_2 and \vec{Z}_2 . In this study, head movements are separated into three non-simultaneous distinct rotations. Each head rotation must be separated into two successive stages in order to simulate real movements: downward and upward rotation, rotation to the left and then to the right, or tilt toward both shoulders. Hence, three cases are considered:

- case 1: rotation around \vec{Z}_2 , so that $\vec{\omega}_{2/1} = \dot{\gamma}\vec{Z}_2 = \dot{\gamma}\vec{Z}_0$,
- case 2: rotation around \vec{Y}_2 , so that $\vec{\omega}_{2/1} = \dot{\beta}\vec{Y}_2 = -(\dot{\beta} \sin \delta)\vec{X}_0 + (\dot{\beta} \cos \delta)\vec{Y}_0$,
- case 3: rotation around \vec{X}_2 , so that $\vec{\omega}_{2/1} = \dot{\alpha}\vec{X}_2 = (\dot{\alpha} \cos \delta)\vec{X}_0 + (\dot{\alpha} \sin \delta)\vec{Y}_0$.

According to the law of velocity composition, absolute head angular velocity relative to the coordinate frame R_0 is defined by $\vec{\omega}_{2/0} = \vec{\omega}_{2/1} + \vec{\omega}_{1/0}$. Expressions of these two vectors are listed in table 1. The computed angular velocity vector is then applied to the transfer function of each canal to yield cupula displacements.

	Rotation vector $\vec{\omega}_{2/0}$
Case 1	$\vec{\omega}_{2/0} = (\dot{\gamma} + \dot{\delta})\vec{Z}_2$
Case 2	$\vec{\omega}_{2/0} = -\dot{\delta} \sin \delta \vec{X}_2 + \dot{\beta}\vec{Y}_2 + \dot{\delta} \cos \delta \vec{Z}_2 = -\dot{\beta} \sin \delta \vec{X}_0 + \dot{\beta} \cos \delta \vec{Y}_0 + \dot{\delta}\vec{Z}_0$
Case 3	$\vec{\omega}_{2/0} = \dot{\alpha}\vec{X}_2 + \dot{\delta} \sin \delta \vec{X}_2 + \dot{\delta} \cos \delta \vec{Z}_2 = \dot{\alpha} \cos \delta \vec{X}_0 + \dot{\alpha} \sin \delta \vec{Y}_0 + \dot{\delta}\vec{Z}_0$

Table 1: expressions of the rotation and velocity vectors in R_2 and R_0 .

3.3 Simulink model

The global functioning of the Simulink model is explained in Figure 3. The motions experienced by the subject, i.e both the rotational motion of the chair and the

potential head movements, are first implemented using a graphic user interface (GUI). Equations of motion are then solved using the aerospace blockset available in Matlab/Simulink [15]. Finally, the state of each sensor is derived in real time according to their transfer function. In addition, a 3D animation has been programmed to visualize the movements of the sensors, and more particularly the displacement of the cupulas (Figure 4). The parameters of the model are for instance the angular velocity of the chair, the magnitudes of the rotating movements of the head, six instants giving the starting signal of each head movement, the Euler angles defining the coordinate system attached to the canals, etc.

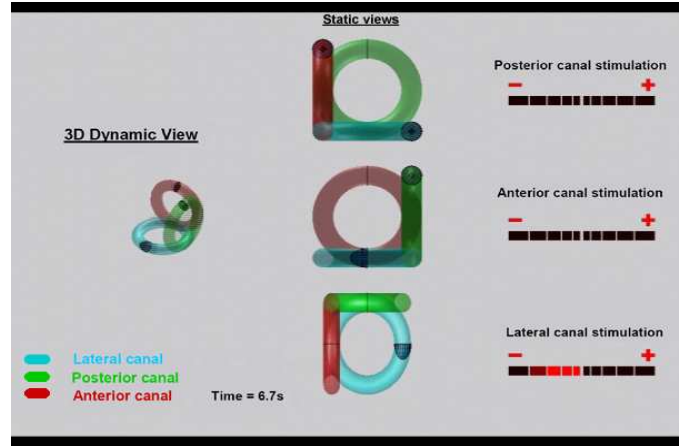


Figure 4: 3D visualization of the semicircular canals and the cupulas. In the dynamic view, the 3 canals are rotating according to the head rotation. The static views allow to observe the cupulas motions in real time. A “positive” motion means that the sensor is excited while a “negative” motion means that the sensor is inhibited.

These values clearly show that the canals do not define an orthogonal coordinate system. In physical sense that means if the head rotates around the perpendicular axis of one canal, not only this canal but the others will be stimulated. Thus, we can conclude that for any rotation of the head, all the angular sensors should provide a stimulus. The component of any vector is therefore defined in the coordinate system attached to the canals according to the transformation matrix:

$$\mathbf{M} = \mathbf{M}_\varphi \mathbf{M}_\theta \mathbf{M}_\psi = \begin{pmatrix} c\theta_a c\psi_a & c\theta_a s\psi_a & -s\theta_a \\ -c\varphi_p s\psi_p & c\varphi_p c\psi_p & s\varphi_p \\ c\varphi_l s\theta_l & -s\varphi_l & c\varphi_l c\theta_l \end{pmatrix}$$

with $c = \cos$, $s = \sin$.

However it is important to note that each canal admits a specific direction of stimulation, which maximizes the excitation: the lateral, anterior and posterior canals primarily sense yaw, roll and pitch respectively.

\vec{e}_a	$\psi_a \approx 2.212$	$\theta_a \approx 0.177$	$\varphi_a = 0$
\vec{e}_l	$\psi_p \approx 2.336$	$\theta_p = 0$	$\varphi_p \approx -0.274$
\vec{e}_p	$\psi_l = 0$	$\theta_l \approx -0.331$	$\varphi_l \approx 0.038$

Table 2: Euler angles in radian which define the perpendicular of each canal.

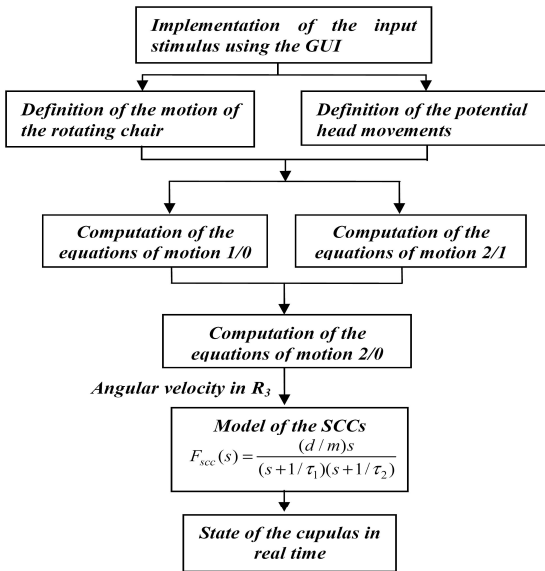


Figure 3: schematic block diagram of the simulink model.

The model takes into account a coordinate frame attached to the canals. Indeed, it is important to determine the components of the angular acceleration vectors in this specific coordinate system as it permits to know whether each canal is stimulated or inhibited. This coordinate frame is derived by using experimental Euler angles, which define the perpendicular of each canal plane $\vec{e}_a, \vec{e}_l, \vec{e}_p$ (anterior, lateral and posterior respectively), i.e their orientation in a 3D space relatively to the head coordinate frame. These angles were determined by several authors and more recently by Della Santina [16]. They are summarized in table 2.

4. SIMULATION RESULTS

4.1 Rotation movement of the chair

This simulation mimics the usual diagnosis procedure of the lateral semicircular canal. During this first experiment the patient is strapped into a rotating chair. His head is kept fixed relatively to the device, and tilted downward of about 25° to bring the lateral semicircular canal in the plane of rotation. A constant angular velocity of $\dot{\delta}=100^\circ/s$, for instance, is then applied to the chair. This motion starts at $t_0=1s$ and achieves its steady state in 1s. This simulation lasts 40 seconds. The volume displacement of the cupula is shown on Figure 5. If the canals are considered to be orthogonal, only the lateral canal is stimulated. At the beginning of the rotation, the endolymph within the lateral canals lags behind due to its inertia. Consequently, the cupula is deflected in the opposite direction of the head rotation (Figure 5a). This deflection causes a sensation of motion. The angular velocity of the chair being sustained at a constant angular rate, the endolymph in the lateral canal tends to catch up with the rotation of the head eliminating the relative movement. Therefore, the cupula returns to its rest position due to its elastic properties, and the sensation of motion ceases.

Figure 5(a) and (b) show the influence of the non-orthogonality of the canals. From those plots we observe a slight displacement of the anterior and posterior cupula that does not appear in the case of an orthogonal system. However, the lateral canal experiences the highest stimulation as its plane is quasi-perpendicular to the axis of rotation. The displacement of the lateral cupula generates a sensation of rotation, which lasts about thirty second according to the imposed angular velocity.

4.2 Rotation movement of the chair and then of the head

The motion of the chair is the same as above. In this case, the subject does a downward and upward head rotation at time $t=10s$ and $t=25s$ respectively. For simplicity purpose, we here consider head rotation of 90° , even though lower magnitude should rather be considered so as to represent physiological head motions. This kind of head motion - during a rotational motion of the chair at a constant rate - elicits the stimulation of the other canals. The displacements of the cupulas can be observed in Figure 5(c) and (d). During the first 10s, the movement of the cupulas is the same as the previous experiment. At time $t=10s$, the subject does a downward head rotation of 90° from the previous head position. In the case of an orthogonal set of canals, this head motion brings the posterior canal into the plane of rotation.

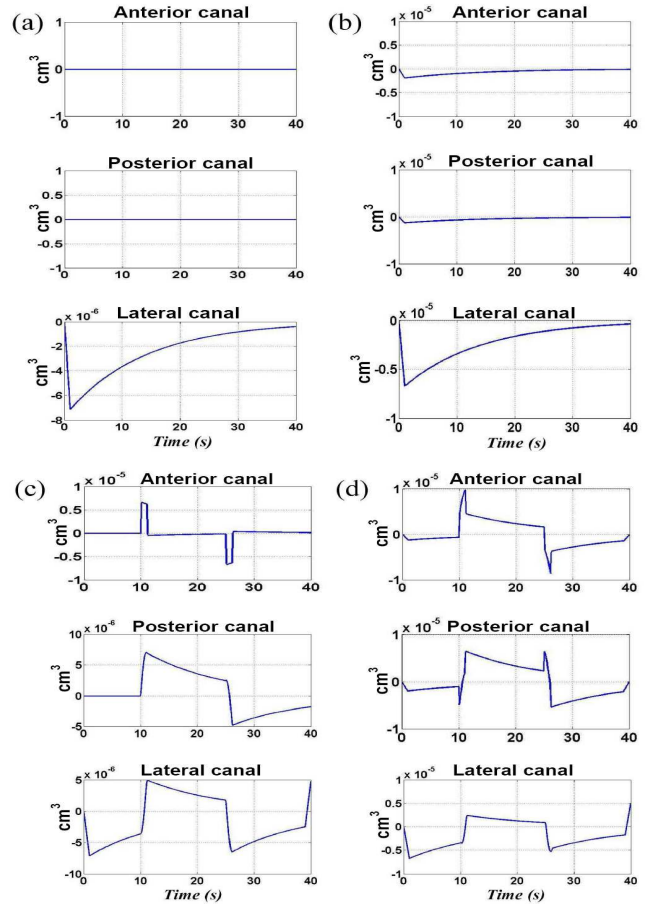


Figure 5: Displacement of the cupula of each canal due to: (a) and (b) rotational movement of the chair; (c) and (d) rotational movement of the chair and of the head. Graphics (a) and (c) correspond to an orthogonal coordinate system R_3 , whereas (b) and (d) correspond to a non-orthogonal coordinate system R_3 . The non-orthogonality of R_3 entails a slight response of the verticals canals. This kind of response might be similar in the case of the existence of coupling terms between the canals due to fluid flow.

Therefore the cupula of the posterior canal is in turn deflected whereas the cupula of the lateral canal bends in the opposite direction as the fluid keeps moving relatively to the wall of the lateral canal. At time $t=25s$, the reverse phenomenon is produced as the subject makes an upward head rotation of the same magnitude.

It can be noticed that the succession of head movements, during a constant rotation of the body, creates erroneous motion sensations known in the aeronautics field as the Coriolis Effect. For example, at $t=10s$ the downward motion of the head engenders a positive displacement of the lateral cupula as the fluid within the canal is still in motion. This means that the subject has a sensation of

rotation opposite to the rotation of the chair. Simultaneously - the anterior and posterior canals being brought into the plane of rotation - a sensation of rotation in the yaw plane relative to the body results. The resulting coriolis illusion experienced is here one rolling and yawing to the right.

CONCLUSION

This model simulates one of the usual tests carried out during a diagnosis of the vestibular sensory system. In addition, several rotation movements of the head can also be taken into account in order to stimulate the vertical canals. The model computes equations of motion in the coordinate system attached to the semicircular canals, which underline the fact that all the canals are stimulated for any rotation. This model also allows getting a better understanding of different kinds of erroneous motion sensations, which can appear during combined rotation motions and might be very interesting in the aeronautical field.

At this moment, the major limitation of this model is that it does not entirely represent the diagnosis procedure of the vestibular system. Currently, the way to explore the vestibular component of the inner ear is to record the vestibulo-ocular-reflex (VOR) during different kind of experiments including the rotary chair test. This reflex is directly linked to the stimulation of the vestibular sensors. By examining this ocular reflex relatively to the imposed rotational movements, the specialists are able to detect any vestibular deficiencies. A potential improvement could be to implement a model of the vestibulo-ocular-reflex (Zupan [17]) to provide theoretical eye movements, which would be then compared with clinical recordings. Another perspective would be to include in the model the functioning of the otolith organs, which sense linear accelerations.

ACKNOWLEDGEMENT

The authors thank Dr J-F. de Lauzun for providing valuable details about the anatomy and physiology of the inner ear. This work was supported by F. Prieur, Integral Design.

REFERENCES

[1] Steinhausen W., *Über die beobachtungen der cupula in der bognegansampullen des labyrinthes des lebenden hechts*, Pflügers Arch. 232, pp. 500-512, 1933.

- [2] Groen J.J., *The semicircular canal system of the organs of equilibrium*, Phys. Med. Biol., pp. 103-117, 1956.
- [3] Van Egmond A.A.J., Groen J.J., Jongkees L.B.W., *The Mechanics of the Semicircular Canal*, J. Physiol., vol. 110, pp. 1-17, 1949.
- [4] Njeugna E, Kopp C.M., *Modèles mécaniques d'un canal semi-circulaire*, J. Biophys. Biomécan. vol. 10, pp. 63-70, 1986.
- [5] Fernandez C, Goldberg J.M., *Physiology of peripheral neurons innervating semicircular canals of the squirrel monkey. II. Response to sinusoidal stimulations and dynamics of peripheral vestibular system*, J. Neurophysiol. vol. 34, pp. 661-675, 1971.
- [6] Oman C.M., Marcus E.N., Curthoys I.S., *The influence of semicircular canals morphology on endolymph fluid flow dynamics*, Acta Otolaryngol. vol. 103, pp. 1-13, 1987.
- [7] Rabbitt R.D., Damiano E.R., Grant J.W., *Biomechanics of the Semicircular Canals and Otolith Organs*, Springer Handbook of Auditory Research, pp. 153-201, 2004.
- [8] Steer R.W., *The influence of Angular and Linear Acceleration and Thermal Stimulation on the Human Semicircular Canal*, M.I.T. Thesis, 1967.
- [9] Van Buskirk W.C., *The fluid mechanics of the semicircular canals*, J. Fluid Mech. vol. 78, pp. 87- 98, 1976.
- [10] Roman S., *Physiologie vestibulaire*, Ency. Méd. Chirurg., Elsevier, 2000.
- [11] Sauvage J.-P., *Anatomie de l'oreille interne*, Ency. Méd. Chirurg., Elsevier, 1999.
- [12] Hillman D.E., McLaren J.W., *Displacement configuration of the semicircular canal cupulae*, Neuroscience, vol. 4, pp. 1989-2000, 1979.
- [13] Rabbitt R.D., *Directional coding of three-dimensional movements by the vestibular semicircular canals*, Biol. Cybern. vol. 80, pp. 417-431, 1997.
- [14] Adenot S., *Artificial gravity: Changing the intensity of Coriolis Cross-Coupled stimulus with head angle*, Master of Science, MIT, 2004.
- [15] Natick, *Simulink User's Guide*, The MathWorks, Inc., March 2007.
- [16] Della Santina C.C., Polyagaylo V., *Orientation of human semicircular canals measured by three dimensional multiplanar CT reconstruction*, J. Assoc. Res. Otolaryngol. vol. 6, pp. 191-206, 2005.
- [17] L. Zupan, *Modélisation du Réflexe Vestibulo-Oculaire et prédiction des cinétoses*, PhD Thesis, Ecole Nationale Supérieure des Télécommunications, ENST95-E004, 1995.